Reduced B12 Uptake and Increased Gastrointestinal Formate Drive Archaeome-Mediated Breath Methane Emission in Humans

Christina Kumpitsch
Medical University of Graz: Medizinische Universitat Graz
Florian Fischmeister
University of Graz: Karl-Franzens-Universitat Graz
Alexander Mahnert
Medical University of Graz: Medizinische Universitat Graz
Sonja Lackner
Medical University of Graz: Medizinische Universitat Graz
Marilena Wilding
University of Graz: Karl-Franzens-Universitat Graz
Corina Sturm
University of Graz: Karl-Franzens-Universitat Graz
Anna Springer
University of Graz: Karl-Franzens-Universitat Graz
Tobias Madl
Medical University of Graz: Medizinische Universitat Graz
Sandra Holasek
Medical University of Graz: Medizinische Universitat Graz
Christoph Hoegenauer
Medical University of Graz: Medizinische Universitat Graz
Ivan Berg
University of Munster: Westfalische Wilhelms-Universitat Munster
Veronika Schoepf
Medical University of Vienna: Medizinische Universitat Wien
Christine Moissl-Eichinger (christine.moissl-eichinger@medunigraz.at)
Medical University Graz https://orcid.org/0000-0001-6755-6263

Research

Keywords: archaeome, microbiome, methanogens, methane, gut, gastrointestinal tract, metabolome, metagenome, Methanobrevibacter, Christensenellaceae

Posted Date: March 22nd, 2021

DOI: https://doi.org/10.21203/rs.3.rs-313313/v1

Abstract

Background

Methane is an end product of microbial fermentation in the human gastrointestinal tract. This gas is solely produced by an archaeal subpopulation of the human microbiome. Increased methane production has been associated with abdominal pain, bloating, constipation, IBD, CRC or other conditions. Twenty percent of the (healthy) Western populations innately exhale substantially higher amounts (>5 ppm) of this gas. The underlying principle for differential methane emission and its effect on human health was still not sufficiently understood.

Results

We assessed the breath methane content, gastrointestinal microbiome, metagenome, metabolome, and eating behavior of one-hundred healthy young adults (female: *n* = 52, male: *n* = 48; mean age =24.1). On the basis of the amount of methane emitted, participants were grouped into high methane emitters (CH4 breath content 5-75 ppm) and low emitters (CH4 < 5 ppm).

The microbiomes of high methane emitters were characterized by a 1000-fold increase in *Methanobrevibacter smithii*. This archaeon co-occurred with a bacterial community specialized on dietary fibre degradation, which included members of Ruminococcaceae and Christensenellaceae. As confirmed by metagenomics and metabolomics, the biology of high methane producers was further characterized by increased formate and acetate levels in the gut. These metabolites were strongly correlated with dietary habits, such as vitamin, fat and fibre intake, host genetics, and microbiome function, altogether driving archaeal methanogenesis.

Conclusions

This study enlightens the complex, multi-level interplay of host diet, genetics and microbiome composition/function leading to two fundamentally different gastrointestinal phenotypes and identifies novel points of therapeutic action in methane-associated disorders.

Full Text

This preprint is available for download as a PDF.

Figures

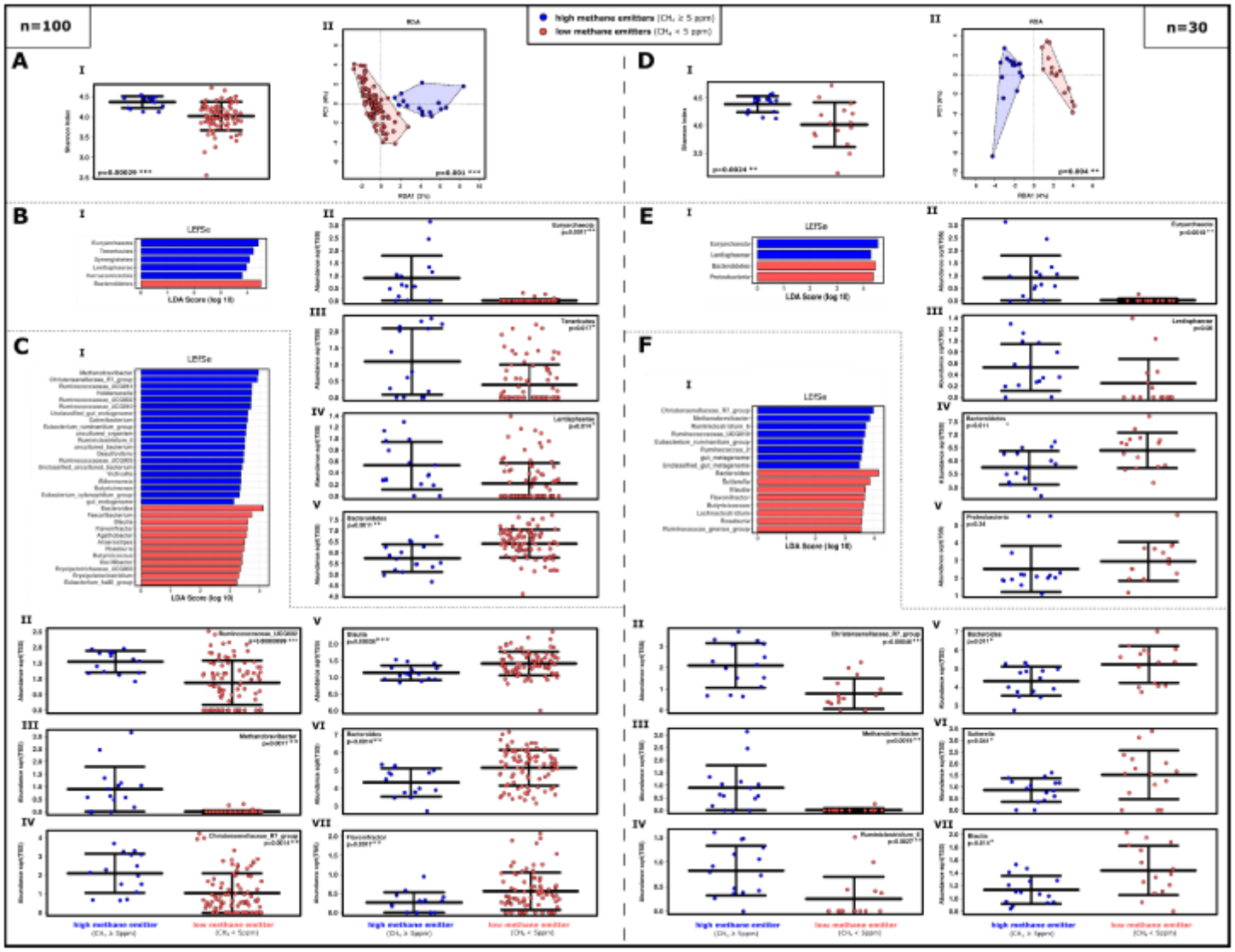

Figure 1

Differences in alpha and beta diversity based on the “universal” approach of 16S rRNA gene sequencing between high (HE) and low methane emitters (LE). A-C. Profiles of the whole study cohort (n=100). D-F. Profiles of the matched subset only (n=30). A.I/D.I. An examination of Shannon diversity index revealed significant differences in alpha diversity (RSV based; ANOVA). A.II/D.II. The microbiome of HEs clustered significantly differently in the RDA plot (RSV based). B.I/E.I. LEfSe analysis of the 100 most abundant phyla and B.II/E.II-B.V/E.V. Relative abundance of selected phyla in ANOVA plots. C.I/F.I. LEfSe analysis of the 100 most abundant genera and C.II/F.II-C.VII/F.VII. ANOVA plots of selected genera.

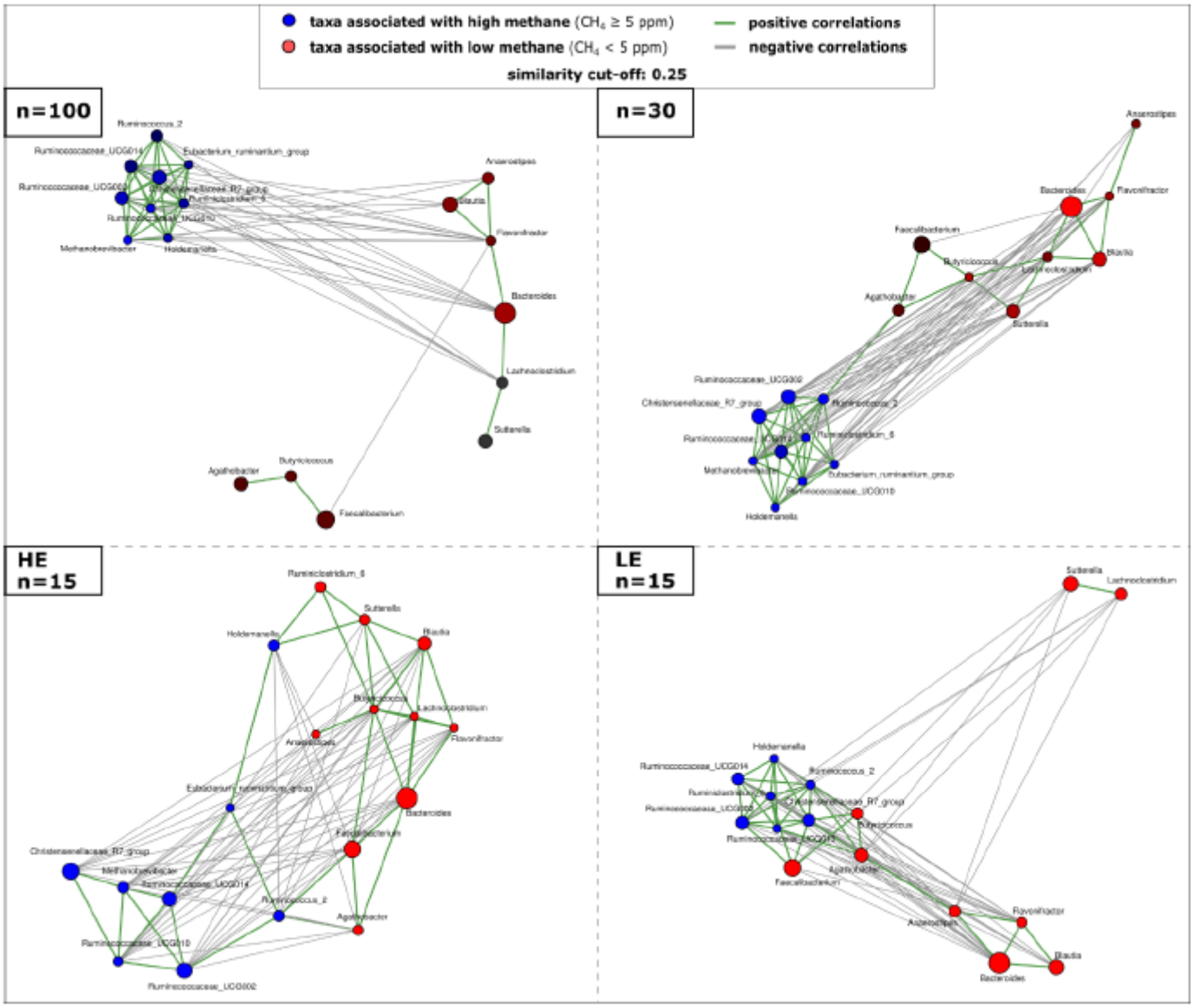

Figure 2

Co-occurrence networks based on Spearman's rho correlation of selected genera in HE and LE microbiome samples. Taxa were selected based on significantly different relative abundances in both sample types and LEfSe analyses. Left, upper panel: Whole study cohort (n=100), right, upper panel: matched study subset (n=30). Lower panels show co-occurrence patterns in the HE (left) or the LE samples (right).

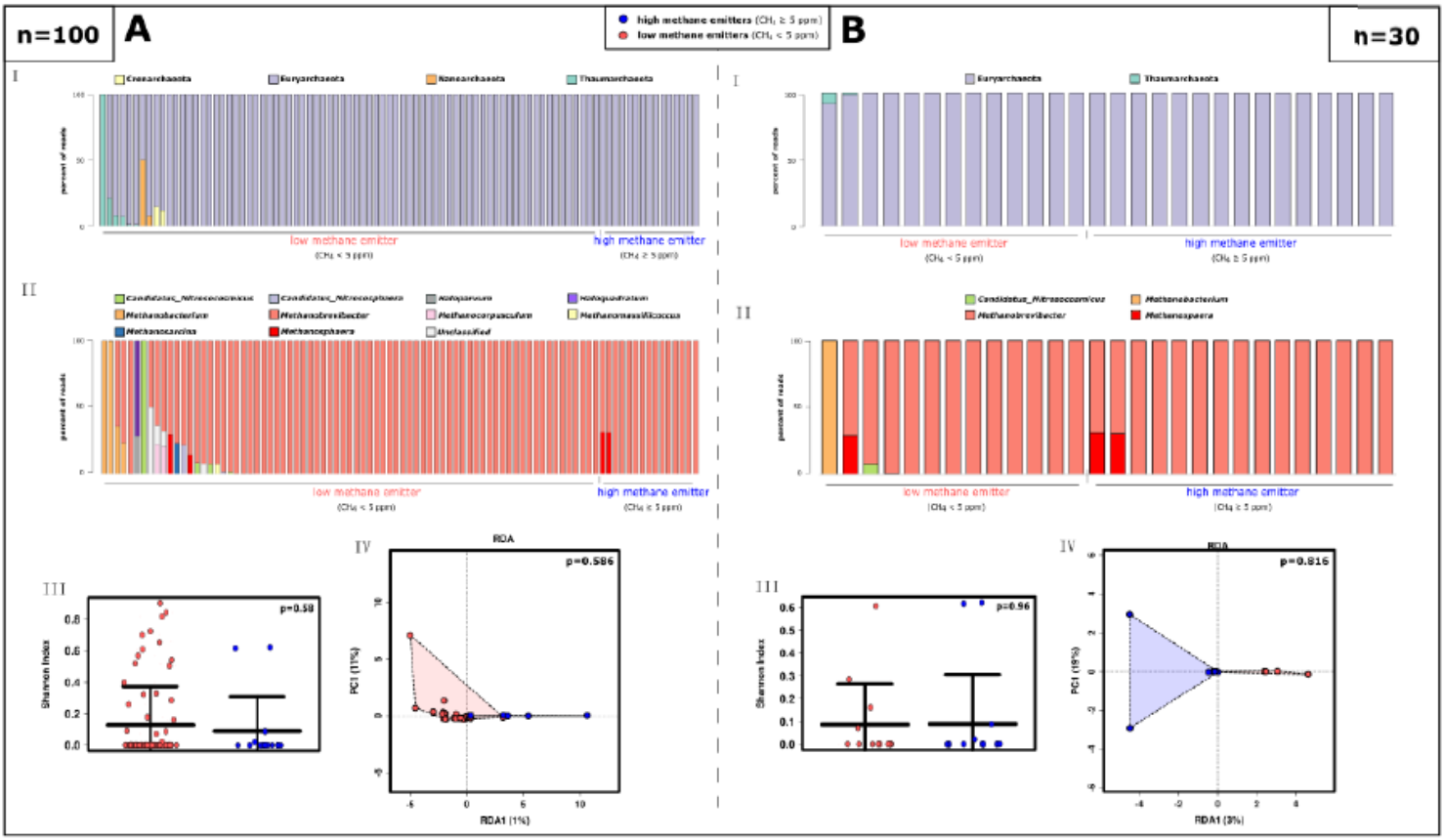

Figure 3

Archaeome profile of HE and LE samples, based on the “archaeal” approach of 16S rRNA gene sequencing. A. Profile of the whole study cohort (n=100). B. Matched study subset (n=30). I. Bar chart of the 20 most abundant taxa compared regarding their low or high methane emission at the phylum level and II. at the genus level. III. Shannon diversity, and IV. RDA plot at RSV level.

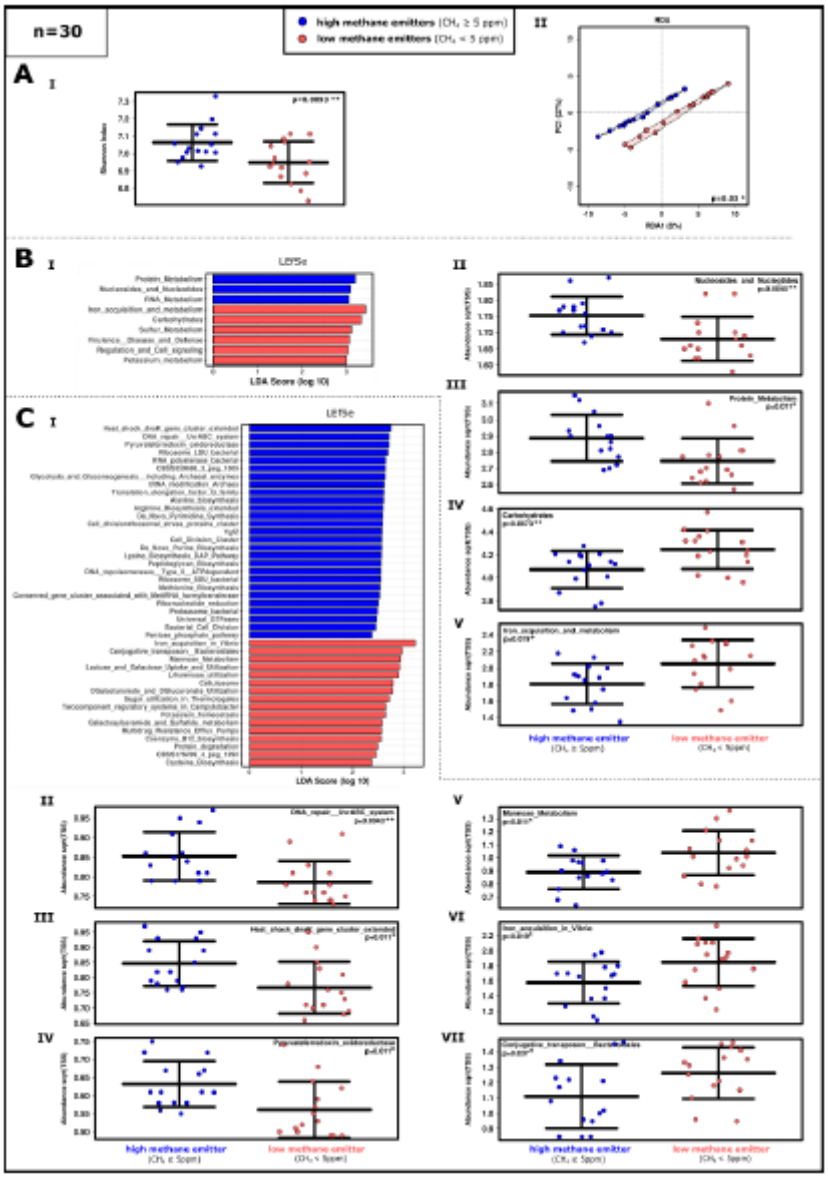

Figure 4

Overview of the divergent functions of the HE and LE based on the shotgun metagenome analysis (subsystems). A.I. Shannon diversity and A.II. RDA plot at feature level. B.I. LEfSe analysis and B.II-.V. ANOVA plots at highest subsystem level (level 1). C.I. LEfSe analysis and C.II-V.II. subsystem at level 3. (100 most abundant; n=30)

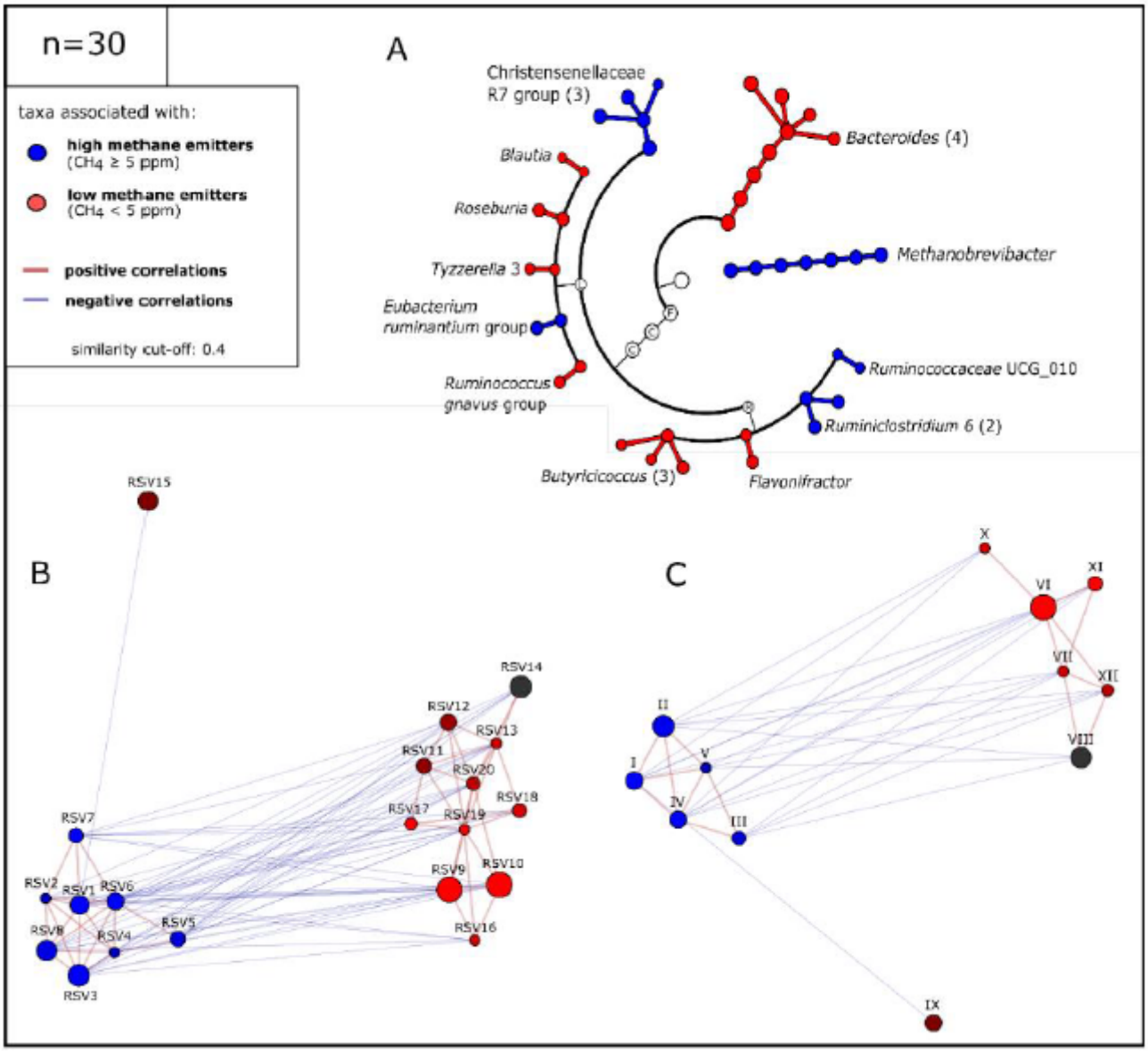

Figure 5

Identified keystone taxa in HE and LE subjects. A. Cladogram of LE and HE keystone taxa. F: Firmicutes, C: Clostridia/Clostridiales, L: Lachnospiraceae, R: Ruminococcaceae. Numbers in brackets indicate the number of contributing RSVs; B. and C. Network of keystone taxa of HE and LE at RSV and genus levels, respectively. I → RSV1: Methanobrevibacter; II→ RSV2-4: Christensenellaceae R7 group; III → RSV5: Eubacterium ruminantium group; IV → RSV6-7: Ruminiclostridium; V → RSV8: Ruminococcaceaea UCG010; VI → RSV9-12: Bacteroides; VII → RSV13: Ruminococcus gnavus group; VIII → RSV14: Blautia; IX → RSV15: Roseburia; X → RSV16: “Tyzzerella”; XI → RSV17-19: Butyricicoccus; XII → RSV20: Flavonifractor (also see Supplementary Table 3)

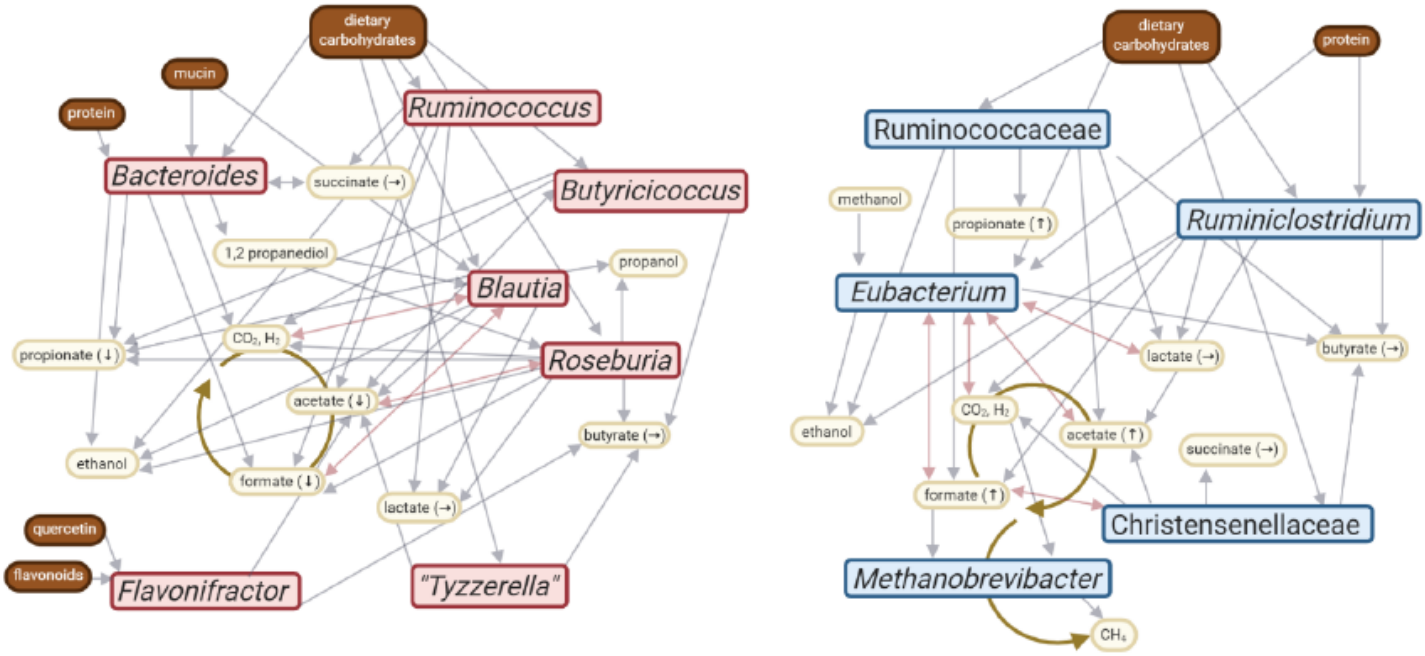

Figure 6

Metabolic network of key-stone taxa in LE and HE microbiomes. Metabolites measured in stool samples are indicated by arrows; respective increase or decrease of the median by >5% is displayed.

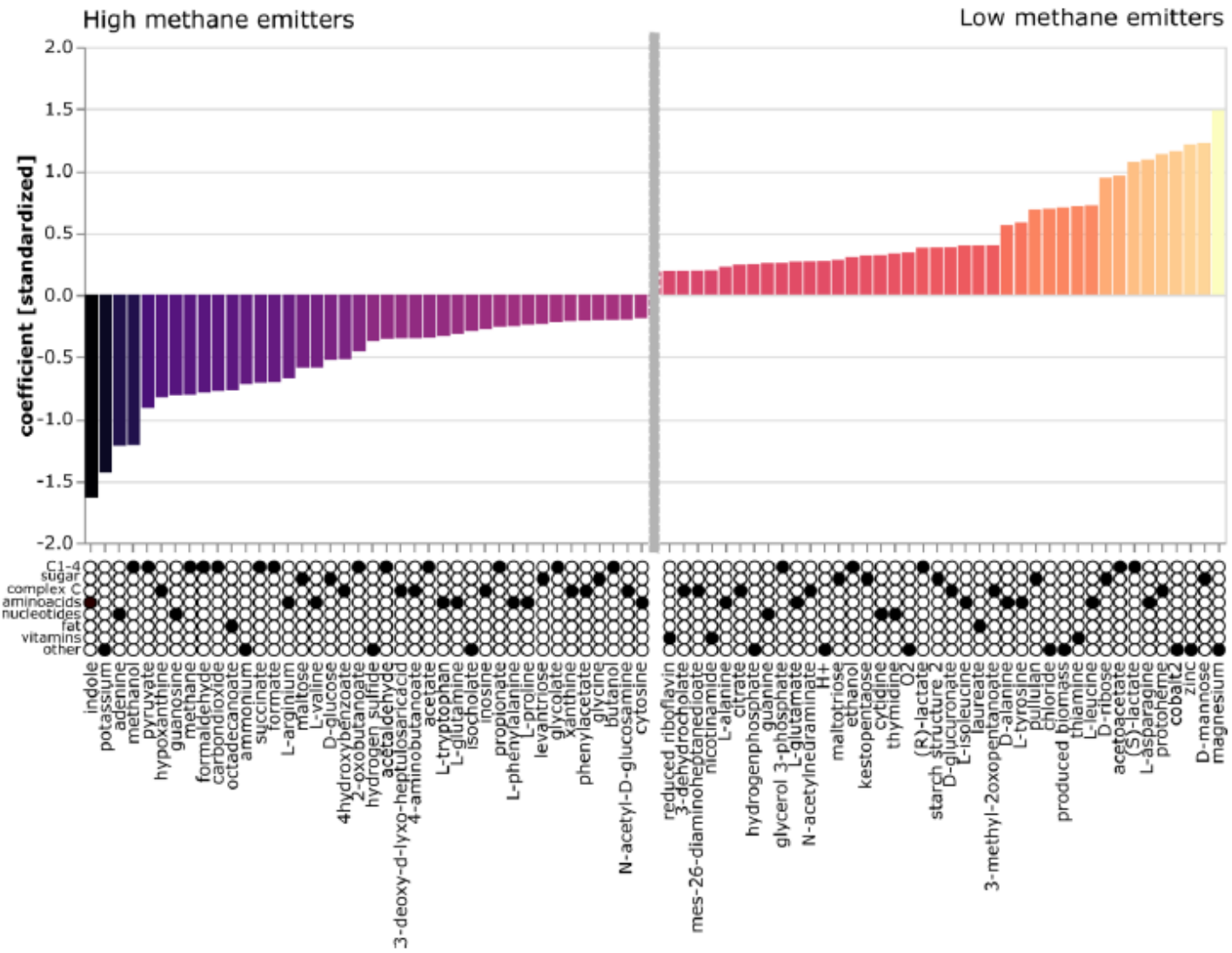

Figure 7

MICOM model-based flux balance analysis of keystone taxa. The 40 most significant metabolites are shown for each condition. Left: HE, right: LE.

Supplementary Files

This is a list of supplementary files associated with this preprint. Click to download.

- 20201221MethanogensSupplementalFigures.pdf
- SuppItem1KronaHELEampliconuniversaln100.html
- SuppItem2KronaHELEampliconarchaean100.html
- SuppItem3KronaHELEmetagenomeSEEDn30.html
- SuppItem4KronaHELEmetagenomeRefSeqn30AB.html
- SuppItem5KronaHELEmetagenomeRefSeqn30A.html

- SupplItem613micomheatmaps.pdf
- SupplementaryDataset17.xlsx
- SupplementaryMethods.docx.pdf
- Supptables16.xlsx